Pulsed Optically Pumped Rb clock

Pulsed Optically Pumped Rb clock

Pulsed Optically Pumped Rb clock

S Micalizio[1], F Levi[1], A Godone[1], C E Calosso[1], B François[1], R Boudot[2], C Affolderbach[3], S Kang[3], M Gharavipour[3], F Gruet[3], G Mileti[3]

[1]Physical Metrology Division, INRIM, Strada delle Cacce 91, 10135 Torino, Italy
[2]Time&Frequency Dpt, FEMTO-ST, CNRS, Université de Franche Comté, Besançon, France
[3]Laboratoire Temps-Fréquence, Université de Neuchâtel, Neuchâtel, Switzerland

Abstract. INRIM demonstrated a Rb vapour cell clock based on pulsed optical pumping (POP) with unprecedented frequency stability performances, both in the short and in the medium-long term period. In the frame of a EMRP project, we are developing a new clock based on the same POP principle but adopting solutions aimed at reducing the noise sources affecting the INRIM clock. At the same time, concerning possible technological applications, particular care are devoted in the project to reduce the size and the weight of the clock, still keeping the excellent stability of the INRIM clock. The paper resumes the main results of this activity.

Corresponding author: s.micalizio@inrim.it

1. Introduction

Development of high stability, low consumption, compact clocks is an important challenge for today's technology, both for space and for ground applications. Several different approaches have been pursued in the last years with interesting results on the short term stability [1]. The pulsed optically pumped (POP) Rb Clock with the possibility to separate in time optical pumping and microwave interrogation, is one of the most promising techniques. In fact, in the pulsed scheme, other than reducing by several orders of magnitude the light shift, it is possible to optimize both the microwave amplitude and the detection laser power to achieve the best signal-to-noise ratio. While several different approaches have demonstrated good short term stabilities in 10^{-13} range at 1s, to our knowledge the only approach that could tame at the same time also the medium-long term stability is the POP.

The first prototype of the POP was developed at INRIM under an ESA contract aimed at identifying possible candidates to replace the passive H-maser currently used for on board Galileo GNSS satellites. A short term stability $\sigma_y(\tau) = 1.7\times10^{-13}\ \tau^{-1/2}$ and a long term drift of 7×10^{-15}/day were obtained with this prototype [2]. Aiming to a further improvement of the clock performances, a new system is being developed taking in particular care the design of the microwave synthesis chain, the thermal stability and uniformity of the Rb cell. Another issue is the overall size of the clock; in this regard, a very compact laser head source has been developed and characterized [3] and a magnetron cavity [4] will be used in the physics package.

In this paper, we will discuss the major causes of noise that affect the short and long term stability of the laboratory prototype of the POP clock and how these effects will be mitigated in the new prototype we are developing.

2. The POP Rb clock: laboratory prototype

The prototype developed at INRIM is based on a pulsed approach in which the clock transition is detected by observing Ramsey fringes on a laser absorption signal. The experimental set-up is represented in figure 1 and is composed of three parts: physics package, optics and electronics. A detailed description of the prototype can be found in [2].

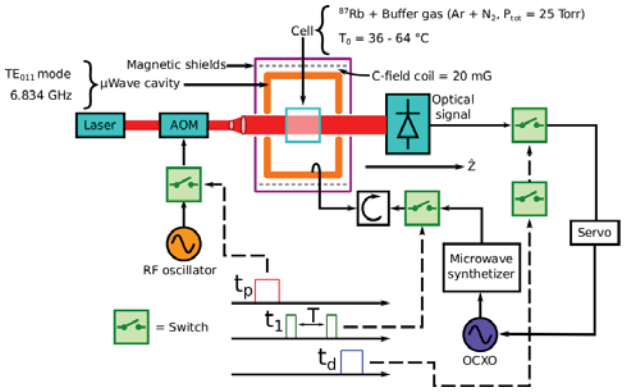

Figure 1. Schematic of the POP clock experimental setup; the timing sequence is also reported; t_p pumping time, t_1 microwave pulse duration, t_d detection time, T free evolution time.

The POP operation is composed of three phases. Initially, the atoms are pumped by a strong laser pulse which generates a large imbalance between the atomic populations of the two ground state hyperfine levels defining the clock transition. Then, the atomic sample experiences two separated microwave pulses according to the Ramsey interrogation scheme. Finally, the atoms that have made the clock transition are detected with a weak laser pulse.
With this approach, Ramsey fringes and frequency stability as those reported in figure 2 have been obtained. A H-maser has been used as a reference in the stability measurement.

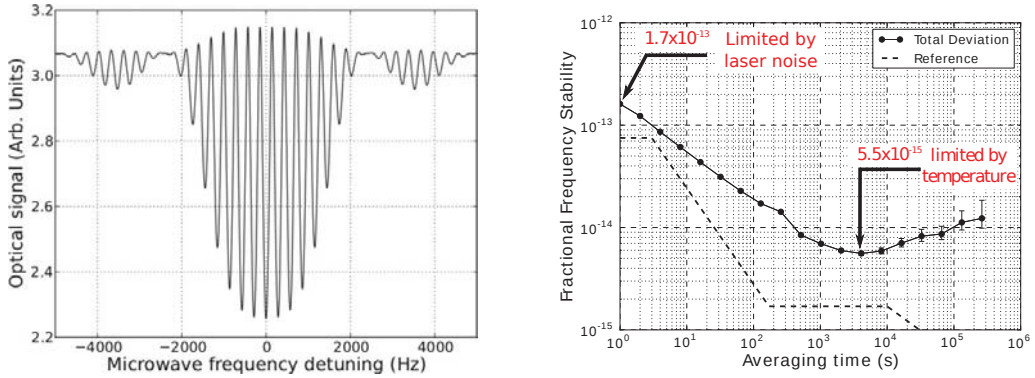

(a) (b)

Figure 2. (a) Ramsey fringes detected in POP clock with optical detection; (b) frequency stability expressed in terms of Allan deviation. The main limiting factors are also reported.

The short-term stability is mainly limited by the transfer of laser noise to the atoms through the PM-AM conversion. The medium long term stability is instead limited by temperature fluctuations.
In next sections we report progress in the development of the new POP clock prototype.

3. Compact cell-cavity system

At the heart of the clock, a Rb vapour cell holds the atomic sample, and is in turn surrounded by a microwave cavity resonator. The microwave resonator serves for applying a well-controlled

microwave field and at the same time acts as a thermal enclosure. Here we describe the cell-cavity system that is based on previous prototypes realized at UniNe-LTF [4] and is currently being assembled. Previous Rb cell realizations for the POP clock had evidenced enhanced temperature sensitivity (ETS) of the clock transition, due to the cells' stem serving as reservoir of atomic Rb [5]. Since the related temperature coefficient $\partial f_{clock}/\partial T_{stem}$ scales proportional to the stem volume, the ETS can be reduced by shrinking the cell stem. The cell used here (see figure 3a) has a diameter and length of 25 mm each, and is filled with ^{87}Rb and an Ar-N_2 buffer-gas mixture (pressure ratio P_{Ar}/P_{N2}=1.6). The cell' stem volume is reduced by more than two orders of magnitude compared to the cells used in [5], resulting in a similar reduction of the ETS. This allows to improve the clock stability and/or to relax the temperature stability requirements for the cell stem. In order to achieve a very compact clock realization, the microwave resonator used to excite the clock transition should add as little additional volume as possible to the cell itself. This is achieved here by a cavity design based on the loop-gap resonator approach, where in our case the resonant structure is formed by six metallic electrodes placed inside a cylindrical conducting shield [3]. This allows to reduce the internal volume of the cylindrical shield to V_{inner} = 28 cm^3, i.e. by more than a factor of three compared to a standard TE_{011} cavity used in previous studies. The outer dimensions of the resonator are 35 mm length by 40 mm diameter, giving an external volume of V_{outer} = 45 cm^3, for a cell volume of V_{cell} = 12 cm^3. The overall design view of this cavity is shown in figure 3b), two cut-off tubes are realize to allow maximum optical clearance whiles avoiding microwave leackage, finally an optical detector unit is directly attached to the cavity. The cavity resonates at the Rb clock transition frequency of ≈ 6.835 GHz, and has a low quality factor; Q≈200. This low Q factor does however not impeach obtaining high-quality Ramsey fringes and thus good clock short-term stability [6], but reduces clock instability contributions relevant on longer time scales arising from cavity pulling or aging of the cavity's resonance frequency.

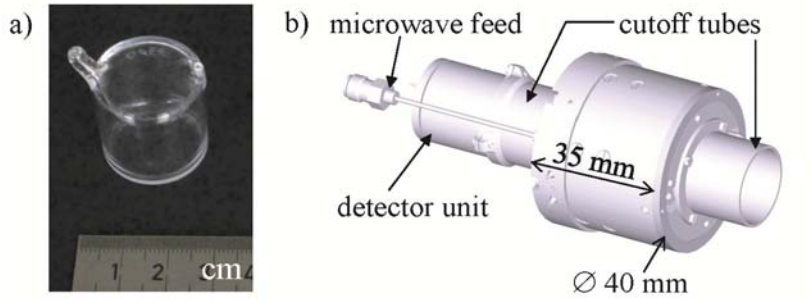

Figure 3. a) Photograph of the Rb vapour cell. The ruler shown indicates centimetres. b) 3D design view of the compact microwave cavity integrating the cell shown in sub-panel a). Both the cell and microwave cavity were designed and realized at UniNe-LTF.

4. Compact laser system

To achieve a compact optical laser system, a stabilized laser head was developed and realized at UniNe-LTF. This laser system includes all optical components required for the clock operation, and notably integrates an acousto-optical modulator (AOM) for fast switching of the optical output, and sub-Doppler spectroscopy optical circuit to lock the laser onto the Rb D_2 transitions observed in a low vapor cell. This laser system has a volume of only 1 litre, and is extensively described in [3].

5. Low-phase noise synthesis chain

In passive atomic clocks (and particularly in the pulsed ones), the interrogation is realized periodically and the control signal of the local oscillator (LO) is updated at equally spaced laps of time. The lack of information caused by the sampling process can lead to a limitation of the short term frequency stability. This effect is known as the intermodulation effect [7] and is coming from the down-

conversion of the LO intrinsic frequency noise at Fourier frequencies higher than the interrogation frequency in the resonator bandwidth. This intermodulation effect is reported for pulsed system as the so-called Dick effect [8] and is a major limitation for high performance vapor cell atomic clocks. The contribution of Dick effect to the clock stability can be evaluated through the equation:

$$\sigma_y^{Dick}(\tau) = \left\{\sum_{k=1}^{\infty} sinc^2\left(k\pi \frac{T}{T_C}\right) S_y^{LO}(k\, f_C)\right\}^{1/2} \tau^{-1/2} \quad (1)$$

where $S_y^{LO}(k\, f_C)$ is the LO power spectral density of the microwave fractional frequency fluctuations and $f_C = 1/T_C$, T_C being the cycle time. Typically, in the POP operation $T_C \approx 4$ ms, so that the phase noise of the LO should be lower than –106 dBrad^2/Hz at $2\, f_C = 2/\, T_C = 460$ Hz to reject the short term frequency limitation of the Dick effect below the 10^{-13} level.

The local oscillator has been designed to be easily adapted also to Cs in a CPT clock. In this case, the synthesis chain deliver a low-phase noise signal at 4.596 GHz (half the Cs clock frequency) suited to drive an electro-optic modulator [9]. In the following parts, only the architecture and the results obtained for Rb synthesis chain are described.

The architecture of the synthesis chain for probing Rb-based vapor cell atomic clocks is reported on figure 4.

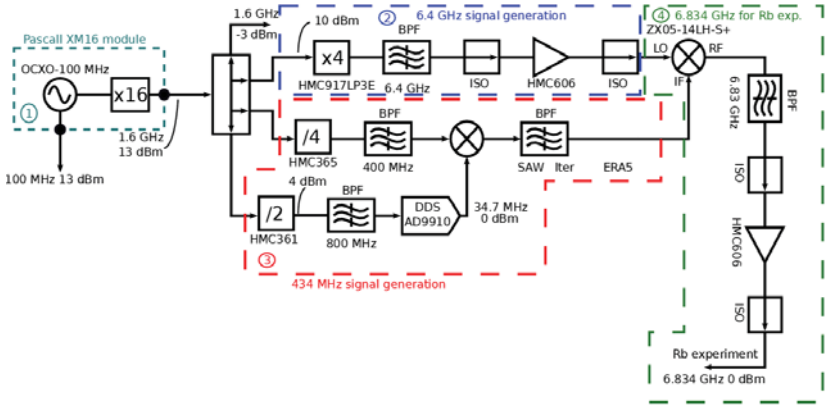

Figure 4. Architecture of the synthesis chain. Four main blocks are identified. 1: XM16 Pascall. 2: Frequency multiplication. 3: Frequency fine tuning. 4: Output signal of the synthesis chain.

The heart of the synthesis chain is the Pascall XM16 module that integrates a 100 MHz oven controlled quartz crystal oscillator (OCXOF-E-100) and its multiplication chain to 1.6 GHz free from excess noise, the latter is sent to a 4-ways power splitter. The 1.6 GHz signal is multiplied to 6.4 GHz by using active frequency multiplier (HMC917LP3E). The resulting signal is then bandpass filtered and amplified (HMC606) drives the LO port of the microwave mixer. The 1.6 GHz signal is also divided to 400 MHz (HMC365) and mixed with the 34 MHz output of the direct digital synthesizer (DDS). The 434 MHz is bandpass filtered by using a surface acoustic wave (SAW) filter. In the last arm, the 1.6 GHz is divided to 800 MHz (HMC361) to provide the clock to the DDS (AD9910). The 434 MHz signal drives the IF port of the microwave mixer. The resulting signal is bandpass filtered, amplified (HMC606), isolated and ready to be used. The DDS provides to the system the fine frequency tuning needed to probe the hyperfine atomic transition, particular attention is paid to the choice of the DDS so that its phase noise does not degrade the performances of the whole multiplication chain. Figure 5 reports the phase noise performances of the synthesis chain.

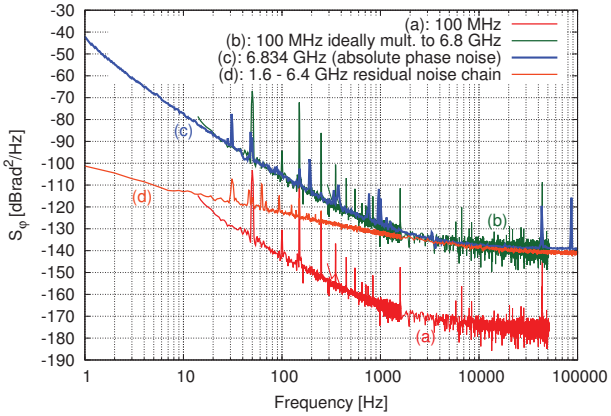

Figure 5. Phase noise performances of the synthesis chain and comparison with reference signals; (b) Dick effect contribution and limitation to the short term frequency.

Curve (a) reports the phase noise measurement of the 100 MHz signal. Particular attention must be paid while measuring the 100 MHz output of ultra low noise OCXOs (such as the Pascall) with a commercial cross-correlation measurement benches, because they do not have a low enough phase noise reference [10] to ensure the right measurement resulting in phase noise measurements exhibiting numerous bump and roll-off (a discrepancy of about 10 dB has been observed). A dedicated bench based on the cross-correlation techniques [11] has then been developed to ensure the right measurement of the OCXO at 100 MHz and at 1.6 GHz (see [12] for more information). The 100 MHz absolute phase noise is measured to be -143 and -174 dBrad^2/Hz at 100 Hz and 10 kHz Fourier frequencies respectively. Curve (c) is corresponds to the absolute phase noise of the 6.834 GHz output and is measured at the level of -105 and -138 dBrad^2/Hz at 100 Hz and 10 kHz offset frequencies respectively. The latter signal performances are then compared to curve (b) corresponding to the theoretical multiplication of the 100 MHz signal to 6.8 GHz, showing that no phase noise degradation occurs during the multiplication process. Curve (e) shows the residual phase noise of the synthesis chain and hence, corresponds to the ultimate phase noise performances achievable using this multiplication chain. Figure 6 reports the Dick effect evaluated according to equation (1) related to the multiplication of the 100 MHz OCXO to 6.34 GHz. On figure 6, the Dick effect is plotted as a function of the noise integration bandwidth. A floor is reached by σ_y once the integrated noise stops to contribute to the total Dick effect. The computation have been achieved by using fitted data. By using the XM16 based synthesis chain, the contribution of the Dick effect to the short term frequency stability has been evaluated at the level of 2×10^{-14}, a value close to the shot noise limit [2].

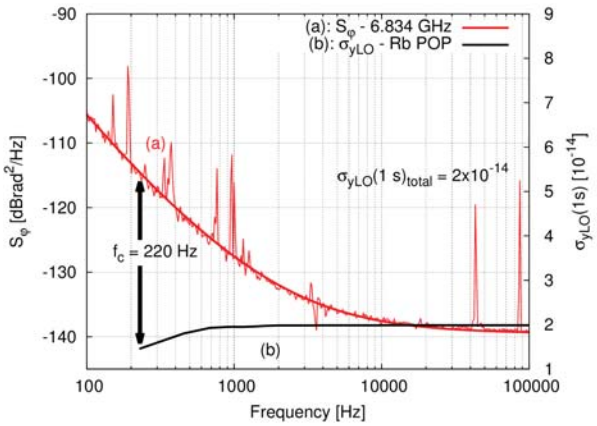

Figure 6. Dick effect contribution and limitation to the short term frequency.

6. Conclusions

The POP clock exhibits very interesting capabilities to be used in those applications where low power consumption, small size, reliability jointly to high frequency stability performances are required. A laboratory prototype has been already implemented and successfully tested at INRIM. The new standard we are going to realize aims at overcoming the limitations of the current prototype and, on the other hand, represents an intermediate step towards the implementation of a commercial device. A particular attention has then been paid to reduce the size, the weight and the power consumption, without losing in stability performances. A commercial prototype of the POP clock would be suitable in many different technological fields, but the features mentioned above make the POP clock particularly suited for space applications, such as GNSS.

Acknowledgments

This work has been funded by the EMRP project IND55 MClocks. EMRP is jointly funded by the EMRP participating countries within EURAMET and the European Union.

Work at LTF was also supported by the Swiss National Science Foundation (SNSF grant no. 140712), and previously by the European Space Agency (ESA) and the Swiss Space Office (Swiss Confederation). The LTF team thanks A.K. Skrivervik, C. Stefanucci, and A.E. Ivanov (EPFL-LEMA), M. Pellaton and T. Bandi for their contributions and collaboration on the cells and cavity.

[1] Godone A, Levi F, Calosso C E and Micalizio S 2015 *Rivista del Nuovo Cimento* **38** 133
[2] Micalizio S, Calosso C E, Godone A and Levi F 2012 *Metrologia* **49** 425
[3] Kang S, Gharavipour M, Gruet F, Affolderbach C and Mileti G 2015 *Proceedings of the joint International Frequency Control Symposium (IFCS) and European Frequency and Time Forum (EFTF),* Denver CO, USA, 800 – 803
[4] Stefanucci C, Bandi T, Merli F, Pellaton M, Affolderbach C, Mileti G and Skrivervik A K 2012 *Rev. Sci. Instrum.* **83** 104706
[5] Calosso C E, Godone A, Levi F and Micalizio S 2012 *IEEE Trans. Ultrason. Ferroel. Frequency Control* **59**, 2646 – 2654
[6] Kang S, Gharavipour M, Affolderbach C, Gruet F and Mileti G 2015 *J. Appl. Phys.* **117** 104510
[7] Kramer G 1974 *Digest of the Conf. on Prec. Electro. Meas.* 157-158
[8] Dick G J 1987 *Proc. Precise Time and Time interval* 133-147
[9] Abdel Hafiz M and Boudot R 2015 *Proc. of the IEEE EFTF-IFCS Conf. Joint Meeting* 71-7
[10] Nelson C W, Hati A and Howe D 2014 *Rev. Sci. Instr.* **85** 024705
[11] Rubiola E and Giordano V 2000 *Rev. Sci. Instr.* **71** 3085
[12] François B, Calosso C E, Abdel Hafiz M, Micalizio S and Boudot R 2015 *Rev. Sci. Instr.* **86** 94707